EUROPEAN FUSION DEVELOPMENT AGREEMENT

EFDA–JET–PR(00)12

M F F Nave et al

Fast Particle Effects on Sawtooth Stability of JET DT Discharges

Fast Particle Effects on Sawtooth Stability of JET DT Discharges

M F F Nave[1], N Gorelenkov[2], K G McClements, S J Allfrey[3], B Balet[4], D N Borba[1], P J Lomas, J Manickan[2], T T C Jones, P R Thomas[5].

EURATOM/UKAEA Fusion Association, Culham Science Centre, Abingdon, Oxfordshire, OX14 3DB, UK

[1]Associação EURATOM/IST, Centro de Fusão Nuclear, 1049-001 Lisbon, Portugal.

[2]Princeton Plasma Physics Laboratory, Princeton, N.J.08543, USA.

[3]Now at CRPP/EPFL, CH-1015 Lausanne, Switzerland

[4]Square de Meuus 8, SDME 1/148, Brussels, Belgium.

[5]Now at DRFC, CEA Cadarache, F-13108 St. Paul-lez-Durance CEDEX, France

ABSTRACT

JET experiments using deuterium and tritium have made it possible to study sawtooth stability in plasmas approaching thermonuclear conditions. Record fusion yields were obtained in discharges where the sawtooth was delayed. In a sequence of discharges designed to study alpha-heating, a new phenomenon was observed: the sawtooth period increases with tritium concentration. The internal kink stability for both high performance and alpha-heating experiment plasmas was studied. Calculations for the record fusion discharge at the time of maximum fusion power (P_{fus} = 16 MW), showed that alpha-particles make a significant stabilising contribution to the potential energy of the m = 1 internal kink instability. The scaling of sawtooth period with tritium concentration implies a dependence on mean ion mass: possible reasons for such a dependence are considered. Calculations of the kinetic fast particle contribution to the kink potential energy indicate that the rise in sawtooth period with tritium concentration is likely to have arisen from two effects: an increase in the slowing down time of the beam ions, which in these plasmas is proportional to the mean ion mass, and an increase in the proportion of beam ions at the full injection energy.

1. INTRODUCTION

JET experiments in the deuterium-tritium campaign of 1997 (DTE1) [1] have made it possible to study sawtooth stability in plasmas approaching thermonuclear conditions. In the hot ion H-mode régime, discharges with Deuterium and Tritium (DT) demonstrated both high fusion yield [2] and significant alpha-particle heating [3]. Record fusion yields were obtained in discharges where the sawtooth was delayed. In a sequence of discharges designed to study alpha-heating, an interesting new phenomenon was observed: the sawtooth period increases with tritium concentration, suggesting that the sawtooth period depends on the mean ion mass [4].

JET plasmas free of Edge Localised Modes (ELMs) are usually obtained in discharges with strong heating by Neutral Beam Injection (NBI). The sawtooth period is observed to increase with NBI power, such that for $P_{NBI} > 12$ MW no large sawtooth crash is usually observed during the ELM-free period. Thus, for high performance plasmas with $P_{NBI} \sim 18$–20 MW, the sawtooth is not usually a problem. However, as the edge stability is improved, such that external kink modes and ELMs are delayed [5], a possible sawtooth crash at a high value of b (the ratio of volume-averaged plasma pressure to magnetic pressure at the magnetic axis) becomes a concern. The critical parameter is normalised β, defined as $\beta_N \equiv aB_t\beta/I_p$, where a is plasma minor radius in m, B_t is toroidal magnetic field in T, β is expressed as a percentage, and I_p is plasma current in MA. For $\beta_N > 1.4$, sawtooth crash post-cursor oscillations lead to saturation of the neutron yield [4]. In the Preliminary Tritium Experiment (PTE) in 1991 the high performance phase of discharges with 10% T, was terminated at $\beta_N \sim 2$ by a sawtooth coupled to a giant ELM [6-7].

A worrying aspect is the sawtooth unpredictability. For instance, an attempt to repeat the best performance sawtooth-free discharge with the Mark I divertor [8] failed due to the appearance of a sawtooth crash in a subsequent, apparently identical, discharge [9]. Difficulties in reproducing sawtooth behaviour have also been encountered in JET high beta ELMy H-mode experiments designed to study neo-classical tearing modes [10].

In the DTE1 experiments, delaying sawteeth was found to be crucial in the quest for high fusion power. In the high performance, higher power discharges with 50% tritium, a combination of NBI and Ion Cyclotron Resonance Heating (ICRH) was used to obtain input powers of the order of 25 MW [11]. Experimentally sawtooth stability in these discharges was increased by the ICRH heating and by careful adjustments of gas fuelling. Modelling described below indicates that alpha-particle stabilisation was also important for these discharges.

The alpha-heating experiments were performed with 10 MW NBI as the sole auxiliary heating source and the DT mixture scanned from 100% D to nearly 100% T. As expected the deuterium reference discharges showed several sawtooth crashes during the ELM-free period. However, in discharges with 50 – 100% tritium the sawtooth period increases and becomes of the same order as the ELM-free period, similar to observations in deuterium pulses at higher powers.

It is generally believed that sawtooth stability depends on the potential energy δW associated with kink displacements whose toroidal and (dominant) poloidal mode numbers are both unity. We have studied internal kink stability for both high performance and alpha-heating experiment plasmas. Our object was two-fold: to estimate the stabilising contribution of alpha-particles to sawtooth stability in the record fusion power discharges and, to consider possible reasons for a dependence of the sawtooth period on the mean ion mass.

2. SAWTOOTH OBSERVATIONS

2.1. High Performance Discharges

Record values of fusion power, P_{fus}, were obtained in high power discharges, with a beam DT mixture of 50% T injected into a plasma background with the same composition. NBI heating ($P_{NBI} \sim 20$ MW) was complemented by ICRH ($P_{ICRH} \sim 3$-5 MW) [10]. Discharges were obtained in two geometric configurations: the so-called standard configuration ($I_p = 3.8$ MA, $B_t = 3.4$ T) and a higher field configuration ($I_p = 4.0$ MA, $B_t = 3.8$ T). The highest fusion power, $P_{fus} = 16$ MW, discussed in Section 4, was obtained in the latter. In both cases q_{95} (the safety factor where the poloidal flux is 95% of its edge value) is equal to 3.5, the average triangularity δ is 0.36, and the boundary elongation κ is 1.8 at the time of maximum fusion power. A complete description of the geometric parameters is given in Ref. [2].

In Figures 1–3 the sawtooth behaviour in three high performance discharges is compared. These discharges were obtained in the standard configuration, where for comparison one

discharge with NBI only was also produced. In all three discharges an early sawtooth is observed ~0.3 s after the heating is switched on. Later on, the discharges all exhibit different sawtooth behaviour.

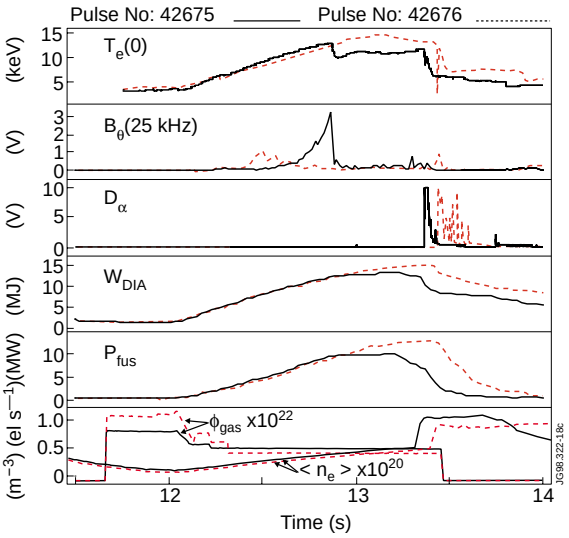

Figure 1: Temporal evolution of similar high performance DT discharges, except for the gas fuelling rate (P_{NBI} = 20MW, P_{ICRH} = 3MW, B_T = 3.4T, I_P = 3.8MA, η_T = 50%).

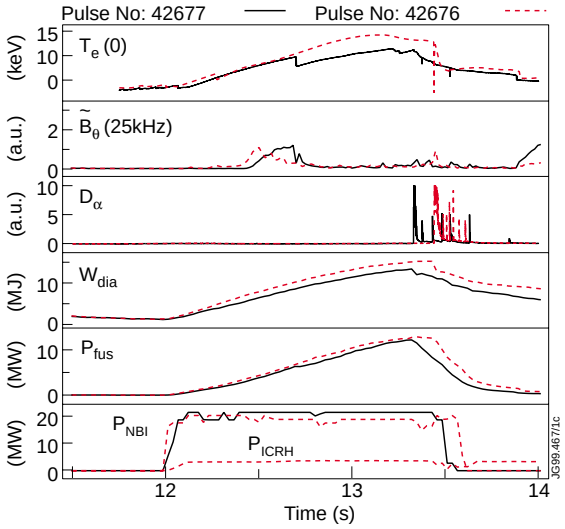

Figure 2: Temporal evolution of similar high performance DT discharges, except for the ICRH heating which was removed in discharge 42677.

In the first discharge in the sequence (42675), a sawtooth crash is observed later in the ELM-free period at β_N = 1.8 (Figures 1 and 3). For the next discharge (42676) gas fuelling was increased. The higher gas rate led to an increase in the time between crashes from 0.6 s to >1.1 s. P_{fus}, which saturated at 10 MW in the discharge with sawtooth period τ_{saw} = 0.6 s, increased to 13 MW in the discharge with improved core stability (high performance in the latter case was terminated by the first giant ELM).

Experience with deuterium-only operation suggested that sawtooth behaviour was sensitive to gas fuelling, and indicated that fine tuning of the gas would be required also in DT. Figure 1 shows the temporal evolution of various quantities in discharges 42675 and 42676: the latter had a slightly higher gas fuelling rate. Fluctuations with toroidal mode number n = 1 are observed in the plasma core in both cases, but the mode dies away in the discharge with higher gas rate, and there is no subsequent sawtooth crash. Gas fuelling is normally carried out in two phases: an initial gas puff before NBI heating, followed by continuous gas injection (gas bleeding) during the heating phase. This improvement in core stability is not understood. Experiments in deuterium indicate that the increased stability is related to the gas puff in the pre-heating phase. This is used to decrease shine-through, improving NBI power deposition into the core of the plasma. However, in the two DT discharges shown, the change in density is very small. There are no significant changes in either the core plasma pressure (calculated with TRANSP) or in the q-profile (reconstructed with EFIT).

In the next discharge in the sequence (42677), ICRH was removed. A sawtooth was again observed (Figure 2). This is consistent with earlier observations that ICRH leads to long sawtooth periods. In early JET experiments with ICRH, these were referred to as “monster sawteeth” [12]. Calculations (discussed below in section 4) show that in these high performance discharges the ICRH fast ions, as well as alpha-particles, make a significant stabilising contribution to the potential energy δW of the internal kink mode with dominant poloidal mode number m = 1.

It is important to note that in the case with NBI only, the sawtooth crash, at β_N~1.2, does not prevent P_{fus} from continuing to rise. In these discharges the sawtooth limitation is not associated with the crash itself but rather with n>2 modes appearing around the time the crash is observed (Figure 3). Magnetic, Soft X-Ray (SXR) and Electron Cyclotron Emission (ECE) fluctuation data show that the sawtooth crash is preceded by long lived m = 1, n = 1 modes with a kink-like structure [4]. The sawtooth crash triggers n = 3 and n = 4 modes outside the q = 1 surface (further work is required to check if those modes are neo-classical tearing modes). Saturation of the plasma stored energy and the neutron yield, coincide with the duration of such post-cursor oscillations. The most dangerous post-cursors in this régime have toroidal mode number n = 3, triggered when β_N~1.8 (Figure 3).

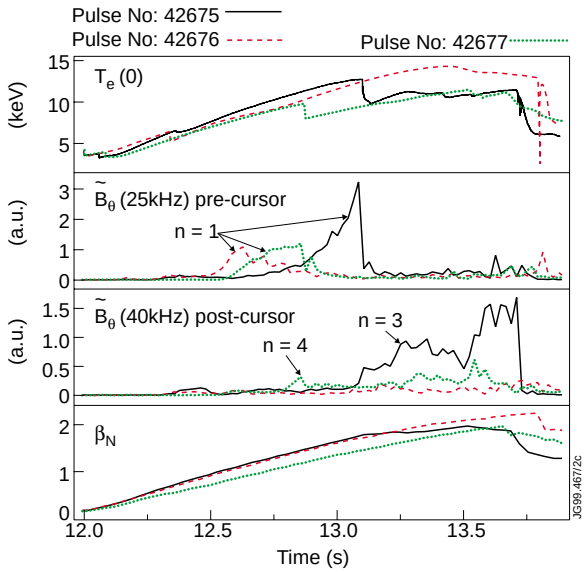

Figure 3: The sawtooth limitation to the discharge depends on the value of ß$_N$. In the JET ELM-free discharges, when ß$_N$>1.4 the sawtooth crash is followed by n>2 modes, likely to be neo-classical tearing modes.

Since at high powers and in a well optimised discharge, i.e. adjusted gas and ICRH heating, the sawtooth period becomes larger than the ELM-free period, it is not possible to compare sawtooth behaviour in the highest performance DT discharges with that in deuterium reference discharges. A study of sawtooth behaviour with different tritium concentrations was, however, possible in the lower power experiments, described in the next section.

2.2. Alpha-heating discharges

The alpha heating experiment consisted of discharges in the standard configuration, with 10 MW of D and T injected by neutral beams into a plasma target with a DT mixture in the same proportions as the NBI. The tritium concentration in these discharges was varied from 0 to 100%, allowing the study of both edge and core MHD stability as a function of the tritium input. In addition a few discharges were produced with 100% tritium injected into a deuterium target plasma and with pure deuterium injected into a tritium background.

The central electron temperature and the D_α emission in Figure 4 show the observed sawtooth and ELM behaviour in discharges with different tritium concentrations, $\eta_T = n_T/(n_D+n_T)$. With increased η_T, the sawtooth period, τ_{saw}, increases, whilst the time of the first giant ELM decreases. Typically, ELMs occur earlier in DT, consistent with the observation of higher edge pedestal pressures. Edge effects observed in the hot-ion H-mode DT discharges are discussed in Refs. [5] and [13]. Figure 5 shows the sawtooth period (solid diamonds) and the fusion power (solid triangles) versus η_T, measured at t = 13.5 s. The fusion power has a non-monotonic dependence on η_T, the maximum P_{fus} occurring when η_T~50%. On the other hand the sawtooth period increases linearly with η_T.

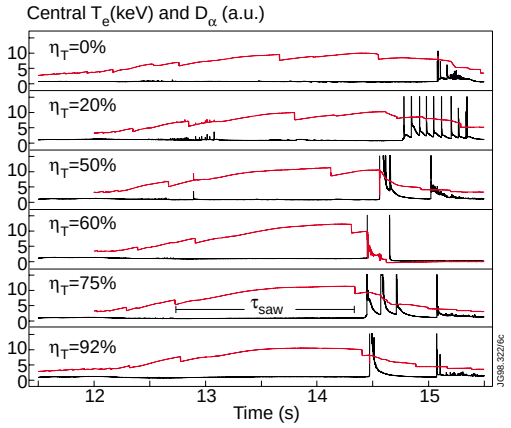

Figure 4: Sawtooth and ELM behaviour in discharges with D and T injected into a DT plasma (P_{NBI} = 10 MW, B_t = 3.4T, I_P = 3.8MA)

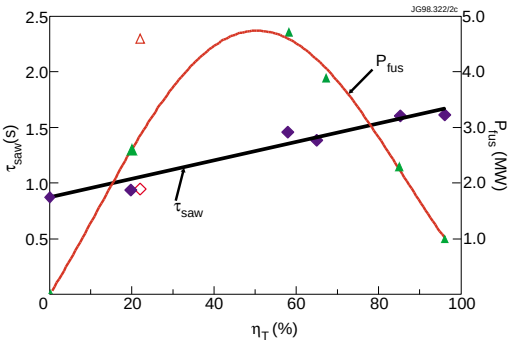

Figure 5: Sawtooth period and fusion power versus core tritium concentration computed using TRANSP [3] at the q = 1 radius for the 6 discharges shown in Figure 4. The open symbols correspond to a discharge where 100% T was injected into a D plasma.

3. THE SAWTOOTH DEPENDENCE ON TRITIUM CONCENTRATION

We consider first the correlation between sawtooth period and tritium concentration observed in the alpha-heating discharges. It is possible that this might be explicable in terms of sawtooth stability criteria based on kinetic and diamagnetic modifications of the MHD energy principle. The stability of the m = 1 internal kink mode, believed to be responsible for the sawtooth crash, depends on the potential energy δW associated with kink displacements. This quantity can be

split into two groups of terms, arising from the core plasma and fast particles: in the case of hot ion H-modes, the core plasma contribution can be further sub-divided into a Magneto-hydro-dynamic (MHD) term and a collisionless thermal trapped ion term, while the fast particle contribution can include terms arising from NBI, ICRH and DT fusion reactions. We thus have

$$\delta W = (\delta W_{MHD} + \delta W_{ki})_{core} + (\delta W_{kNBI} + \delta W_{klCRH} + \delta W_{k\alpha})_{fast} \quad (1)$$

In certain sawtooth models (see e.g. Ref. [14]), a crash is triggered when δW falls below a critical value δW_{crit}.

Since ICRH was not used in the alpha-particle heating pulses, the only energetic ions in these plasmas were alpha-particles and beam-ions. Fusion alpha-particles are expected to make a significant stabilising contribution to the potential energy δW of m = 1 internal kink perturbations in Next Step devices [14]. However, the lack of correlation between P_{fus} and τ_{Saw} (Figure 5) indicates that alpha-particles alone cannot account for the observed variation of τ_{Saw} with η_T. Isotopic effects, which could contribute to the observed dependence of τ_{Saw} on η_T, are found: a) directly in the sawtooth crash threshold conditions [14] through quantities such as: the Alfvén time and the Larmor radius; and b) indirectly through the slowing down time of the beam ions.

In the next three sections these two possibilities are explored. The chosen analysis time for all discharges is t = 13.5 s (i.e. 1.5 s after the beam heating is switched on). This is the time just before the first large sawtooth crash observed in the deuterium reference discharge. Our intention here is not to explain the onset of sawtooth, but rather to look into the relative size of the various components involved in the stability of the internal kink mode as a function of η_T.

3.1. Sawtooth stability threshold

Porcelli and co-authors proposed in Ref. [14] that a sawtooth crash would occur in ITER when any of the following conditions were satisfied:

$$\delta W_{core} < -c_h \omega_{df} \tau_A \quad (2)$$

$$\delta W_{core} + \delta W_{kf} < -\frac{1}{2} \omega_{*i} \tau_A \quad (3)$$

$$c_\rho \hat{\rho} > \delta W > -\frac{1}{2} \omega_{*i} \tau_A \text{ and } s_1 > s_{1crit} \quad (4)$$

Here, the kink energy has been normalised to $2\pi\xi^2 R_0 s_1 \varepsilon_1^2 B_0^2 / \mu_0$, where ξ is the kink displacement, R_0 is the tokamak major radius, $\varepsilon_1 = r_1 / R_0$ is the q = 1 radius normalised to R_0, s_1 is magnetic shear at q = 1, B_0 is the toroidal magnetic field, and m_0 is the free space permeability. The other quantities in Eqs (2)-(4), are all calculated at q = 1 and are defined as follows: τ_A is a characteristic time associated with the Alfvén speed, c_A (the precise definition is $\tau_A = 3^{1/2} R_0 / c_A$),

c_h and c_ρ are dimensionless factors of order unity; $\hat{\rho} = [m_i (T_{i1} + T_{e1})]^{1/2} / eB_0 r_1$, where T_{il} and T_{el} are the ion and electron temperatures; δW_{core} includes the effects of toroidicity, shaping, and kinetic stabilisation by hot thermal ions; δW_{kf} is the kinetic contribution to δW of fast ions (alpha-particles plus beam ions), ω_{df} is a characteristic toroidal precession frequency of those ions; and ω_{*i} is the thermal ion diamagnetic frequency.

In all the discharges considered here there were always fast ions with sufficient energies to ensure that Eq. (2) was not satisfied. The second part of Eq. (4) is equivalent to a condition that s_1 exceeds a critical value [14], which, in the alpha-particle heating pulses, can be estimated to be typically 0.6. Equilibria obtained using the EFIT code [15] indicate that s_1 was typically about 0.4 in these discharges. Equation (3) is the sawtooth instability criterion found to be most relevant to those discharges. This identifies an isotope effect on sawtooth stability arising from the Alfvén time that increases as $m_i^{1/2}$, and so the critical δW for instability becomes more negative as the plasma tritium fraction increases.

The parameters determining δW_{core} (the q-profile, the total plasma beta poloidal, β_p, the plasma shape, and the bulk ion temperature, T_i) did not vary significantly from shot to shot (except in the discharge with 100% T which had a lower s_1 and an atypical m = 1 mode displacement). Here, we do not attempt to evaluate δW_{core}, since in most of the discharges analysed it had approximately the same value, and we are concerned principally with changes in δW and the threshold for instability resulting from an increase in the beam tritium fraction. In the following sections we outline the methods used to calculate the alpha-particle ($\delta W_{k\alpha}$) and beam ion (δW_{kNBI}) contributions to δW_{kf}.

3.2. Stabilisation by fast ions

The alpha-heating discharges were analysed using the transport code TRANSP [16-17]. Figure 6 shows the perpendicular energy density $u_\perp$ of energetic ions in the plasma centre for a particular time (t = 13.5 s) in each of the alpha-particle heating pulses plotted versus the sawtooth period. A strong correlation between $u_\perp$ and τ_{Saw} is apparent. This appears to be very strong evidence for sawtooth stabilisation by fast ions. The only energetic ions in these plasmas were alpha-particles and beam ions. The largest contribution to $u_\perp$ comes from the beam ions. The maximum contribution to $u_\perp$ from alpha-particles is about one third of the beam ion component in the discharge with η_T~60% (Figure 7). Thus, it appears that alpha-particles may be contributing to the stabilisation process (the correlation between τ_{Saw} and $u_\perp$ is less clear-cut if the alpha-particle contribution to the latter is neglected), nevertheless that contribution is small. If a species is isotropic, it is straightforward to show that the perpendicular energy density is equal to twice the parallel energy density, and that the corresponding particle pressure is equal to $u_\perp$. Although beam ions at JET are generally anisotropic, TRANSP results for these discharges at t = 13.5 s indicate that $u_\perp \approx 2\, u_{||}$. As noted above, the beam power is the same (10 MW) in all the

alpha-heating discharges. The highest birth energies E_0 of deuterons and tritons are also approximately identical (in the range 138-155 keV), although a certain fraction of the ions are born at energies $E_0/2$ and $E_0/3$ [18]. The proportion of ions born at the highest energy is significantly higher in the case of tritons than it is in the case of deuterons.

For sufficiently high injection energies (such that the slowing-down is mainly on electrons), the beam ion pressure depends critically on the slowing-down time [19]

$$\tau_{s(NBI)} = \frac{3\pi^{3/2}\varepsilon_0^{\,2} m_e \overline{m}_b v_e^{\,3}}{Z_b^{\,2} e^4 n_e \ln\lambda} \qquad (5)$$

where ε_0 is the free space permittivity, m_e is the electron mass, $\overline{m}_b$ is the average beam ion mass, v_e is the electron thermal speed, Z_b is the beam ion atomic number, e is the proton charge, n_e is the electron density, and $\ln\lambda$ is the Coulomb logarithm. In the alpha-particle discharges the beam ions and the plasma background have the same DT mixture, and therefore $\overline{m}_b = \overline{m}_i$, the average ion mass. Thus, in these discharges $\tau_{s(NBI)} \propto \overline{m}_i$.

The beam ion energies were comparable to or less than the critical energy E_c at which ion-electron and ion-ion collisions are equally important [19]:

$$E_c = 1.48 T_e \left[\frac{A^{3/2}}{n_e} \sum_j \frac{n_j Z_j^2}{A_j} \right]^{2/3} \text{keV}, \qquad (6)$$

where T_e is electron temperature in keV, A is the beam ion mass number, and the summation is over bulk ion species, with n_j, Z_j and A_j respectively denoting density, atomic number and mass number. It can be seen that E_c scales as $m_b / m_i^{2/3}$. At energies $E > E_c$ beam ions slow down predominately on electrons, and the steady-state beam pressure p_b is of the order of the injected power per unit volume, ρ_{NBI}, times $\tau_{s(NBI)}$. The beam pressure in this case scales linearly with the beam ion mass. For $E << E_c$, on the other hand, the beam ions slow down predominately on bulk ions, and undergo significant pitch angle scattering. Using the result that the steady-state beam ion distribution varies as $\tau_{s(NBI)}/(E^{3/2}+E_c^{3/2})$ [19], it is straightforward to show that the beam ion pressure in this regime scales as $\rho_{NBI}\tau_{s(NBI)}(E_0/E_c)^{3/2}$ where E_0 is the beam injection energy. For fixed values of ρ_{NBI} and E_0, and a plasma with $\overline{m}_b = \overline{m}_i$, this would imply $p_b \propto \overline{m}_b^{1/2}$. Since δW_{kNBI} scales approximately with the fast particle pressure [14], it follows that δW_{kNBI} should increase with the plasma tritium fraction.

In the case of the experiments discussed here, E_0 is comparable to E_c, and so for fixed ρ_{NBI} and E_0 one would expect to find a variation of beam pressure with ion mass which was intermediate between that predicted for the supercritical ($E > E_c$) and sub-critical ($E << E_c$) regimes.

In fact, the beam component of $u_\perp(0)$ is about 80% higher in the discharge with 100% tritium beam injection than it is in the discharge with 100% deuterium injection. This strong variation of beam pressure appears to be due partly to the fact that, as noted above, a higher proportion of tritons than deuterons are born at the full injection energy: in the sub-critical regime p_b increases with both $\tau_{s(NBI)}$ and E_0. Small differences in beam injection energies and angles may also have contributed to the variation of p_b with $\overline{m}_b$. In Figures 5 and 6 a discharge with 100% T injected into a deuterium target plasma is shown for comparison. The fact that the sawtooth period in this discharge is similar to that observed in discharges with mainly deuterium (Figure 5) appears at first to contradict the hypothesis that the sawtooth stabilisation in the alpha-heating discharges is related to the ion mass. It is clear from Figure 6 that $u_\perp(0)$ for this discharge is similar to the values calculated for DT discharges with low η_T values and similar sawtooth periods. (This is due to large differences in density and temperature profiles). Thus this discharge does not contradict the hypothesis that the beam ions may be in large part responsible for the sawtooth stabilisation observed in the alpha-particle heating discharges.

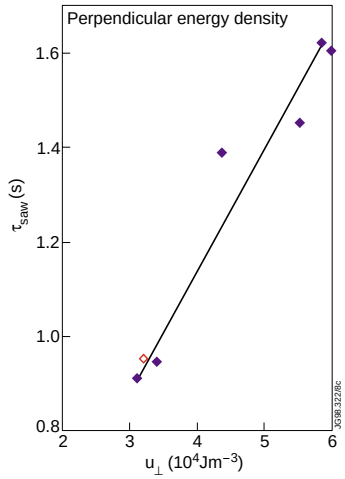

Figure 6: The sawtooth period τ_{saw} versus the central $\mu_\perp$ calculated with TRANSP at t = 13.5 s. The solid line shows the best linear fit to the data. The open symbol corresponds to a discharge in which 100% T was injected into a D plasma.

3.3. Fast particle contributions to the internal kink energy

We have computed δW_{kNBI} and $\delta W_{k\alpha}$ for the alpha-heating discharges using two methods: numerically, using the NOVA-K code [20]; and semi-analytically, using a simplified model developed in Ref. [19]. We start with the semi-analytical calculations. As noted previously, radial profiles of $u_\perp$ and $u_{||}$ for the various energetic ion species in the alpha-particle heating series of discharges indicate that the relation $u_\perp \approx 2u_{||}$ generally holds. This is consistent with the energetic ion distributions being approximately isotropic. To simplify the analysis, we assume that this condition holds, and that $u_\perp$ is thus approximately equal to the particle pressure p. We assume also that the fast ions have slowing-down energy distributions and exponential radial profiles. The alpha-particle and beam ion distribution functions F_α, F_b are thus assumed to be of the form [19].

$$F_\alpha \propto \frac{e^{-r/\Delta_\alpha}}{E^{3/2} + E_{c\alpha}{}^{3/2}} \qquad (7)$$

$$F_b \propto \frac{e^{-r/\Delta_b}}{E^{3/2} + E_{cb}{}^{3/2}} \qquad (8)$$

where $E_{c\alpha}$, E_{cb} are the critical energies of the two species, and the e-folding lengths Δ_α, Δ_b are typically about 0.4 – 0.45 m in the alpha-particle heating pulses. The use of a simple slowing-down distribution is more accurate in the case of alpha-particles than it is in the case of beam ions since, as noted previously, a significant proportion of the latter are born at one half and one third of the maximum injection energy. However, in the isotropic limit the shape of the fast particle energy distribution affects the kink energy only through finite orbit width effects [21], which are relatively small at beam ion energies. As indicated by Eq. (6), the critical energies in Eqs (7) and (8) have a weak dependence on mean ion mass: for simplicity, we set $\overline{m}_i$ equal to 2.5 times the proton mass m_p in both critical energies, and the beam ion mass also equal to 2.5 m_p in E_{cb}. Taking finite orbit width into account, and adopting the distribution given by Eq. (7), the appropriate expression for $\delta W_{k\alpha}$ is [21]

$$\delta W_{k\alpha} = \frac{\beta_{0\alpha}}{(2\varepsilon_1)^{1/2} s_1} \frac{r_1}{\Delta_\alpha} \int_0^1 x^{3/2} e^{-r_1 x/\Delta_\alpha} d_x \int_0^1 \frac{E^{3/2} dE}{E^{3/2}+E_{c\alpha}{}^{3/2}} (1 - \tfrac{1}{2}[1-\kappa_*{}^2(E)]) / \int_0^1 \frac{E^{3/2} dE}{E^{3/2}+E_{c\alpha}{}^{3/2}}. \qquad (9)$$

The integration here is over energy and minor radius, normalised respectively to the alpha-particle birth energy (assumed to be unique and equal to 3.5 MeV) and r_1. The reciprocal of an energy integral appears in order to ensure that the alpha-particle pressure is correctly normalised. The quantity β_{0a} is the central toroidal alpha-particle plasma beta, and

$$\kappa_*{}^2 = \min\{r_1{}^2 \Omega_\alpha{}^2 \varepsilon_1 x (1-x)^2 / 4E_* q^2, 1\}, \qquad (10)$$

where Ω_α is the alpha-particle cyclotron frequency and E_* is now particle energy per unit mass. In general, the radial integral in Eq. (9) includes additional terms of order 1 - q and s (local magnetic shear), which we have neglected. These additional terms have the effect of increasing $\delta W_{\kappa\alpha}$ [22]. Taking the limit of zero orbit width ($E_* \rightarrow 0$, $k_*{}^2 \rightarrow 1$ for all x), Eq. (9) reduces to an expression which, to zeroth order in 1 - q and s, agrees with those used in previous studies (see, for example, Ref. [22]). The appropriate expression for δW_{kNBI} is of exactly the same form as that given by Eq. (9).

To evaluate $\delta W_{k\alpha}$ and δW_{kNBI} for the alpha-particle heating series of discharges, we set r_1 = 0.37 m. According to q-profiles obtained using EFIT, the q = 1 radius lies close to this value at 1.5 s after the start of neutral beam injection in every case. The e-folding lengths of the energy density profiles computed using TRANSP do not vary greatly from shot to shot either, although in general the beam ions have a slightly broader energy density profile than the alpha-particles.

In every case we set $\Delta_\alpha = 0.4$ m and $\Delta_{NBI} = 0.46$ m. Since we are identifying $u_\perp$ with pressure, it follows that $\beta_{0\alpha} = 2\mu_0 u_{\perp\alpha}(0)/B_0^2$ and $\beta_{0b} = 2\mu_0 u_{\perp b}(0)/B_0^2$ (the subscript b referring once again to beam ions). Finally, for the purpose of evaluating the critical δW for a sawtooth crash ($\delta W_{crit} \int -\omega_{*i}\tau_A/2$), we assume that the electron and ion temperatures vary as 1-r/a and that the ion density has a flat radial profile. We set $s_1 = 0.4$, central electron temperature $T_{e0} = 10$ keV, central ion temperature $T_{i0} = 14$ keV, and central ion density $n_{i0} = 3 \times 10^{19} m^{-3}$. Finally, we evaluate $\overline{m}_i$ using

$$\overline{m}_i \equiv \frac{m_T n_T + m_D n_D}{n_T + n_T} = [3\eta_T + 2(1-\eta_T)]m_p. \qquad (11)$$

Circles, squares and triangles in Figure 8 show $\delta W_{k\alpha}$, δW_{kNBI} and $\delta W_{crit,}$ respectively, for the alpha-particle heating discharges. As expected, $\delta W_{k\alpha}$ is highest in a discharge with approximately equal amounts of deuterium and tritium (42847). The relation between δW_{kNBI} and τ_{saw} is not as clear-cut as that between $u_\perp$ and τ_{saw} (Figure 6), but the general trend is for δW_{kNBI} to increase with sawtooth period. Comparing, for example, the discharges with $\tau_{saw} = 1.388$ s and $\tau_{saw} = 1.607$ s, one can see that in the latter case a lower $\delta W_{k\alpha}$ is accompanied by a much higher δW_{kNBI}, the result being a strong increase in kink stabilisation which is consistent with the increase in sawtooth period. It is also apparent from Figure 8 that the isotopic variation of δW_{crit} is much weaker than the variation in either $\delta W_{k\alpha}$ or δW_{kNBI}.

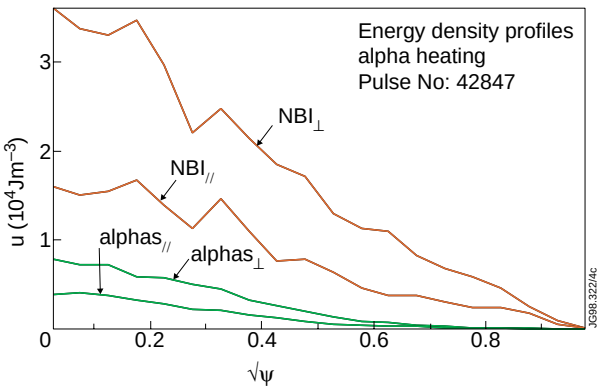

Figure 7: Profiles of beam and alpha-particle energy density computed using TRANSP for t = 13.5 s in alpha-heating discharge 42847, with 60% T.

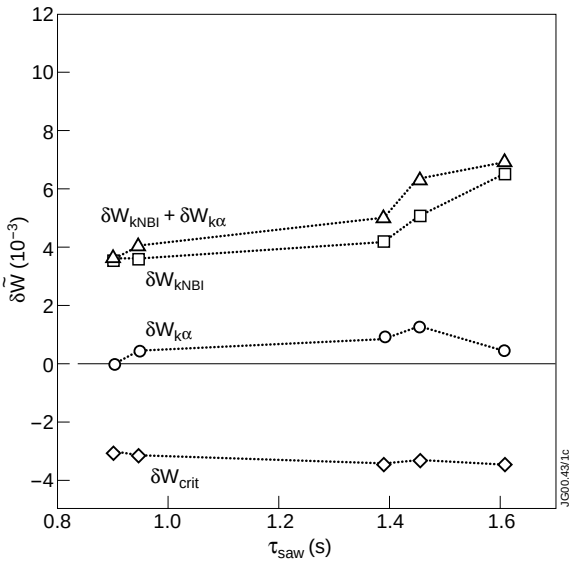

Figure 8: The open symbols show the calculated δW_{crit}, δW_{ka} and δW_{kNBI} versus the sawtooth period in the analytic approximation

A similar pattern emerges from the numerical treatment. We used a recently modified version of NOVA-K which takes into account the finite orbit widths and finite Larmor radii of the fast particles [23] in evaluating the kinetic contribution from the various fast particle groups to the

MHD quadratic form of the mode energy δW_{kf}. It uses a perturbative method with the unperturbed m = 1/n = 1 ideal kink eigenmode structure calculated by the ideal MHD code NOVA [20]. NOVA-K utilises this mode structure to calculate the fast particle contribution δW_{kf}. The NOVA-K code uses TRANSP results for plasma and fast particle parameters. The fast particles were assumed to have slowing-down speed distributions, as in the semi-analytical calculation, while the pitch angle distributions were taken to be isotropic in the case of alpha-particles and Gaussian in the case of NBI ions, peaked at $\lambda = E_{\perp} B_0 / EB = 0.3$, where $E_{\perp}$ is the particle perpendicular energy, and having a broad half width $\Delta\lambda = 0.7$, so that there is a significant fraction of trapped particles. Such a form was chosen to fit the TRANSP results for the tangentially injected beam. Note that the broadening of the pitch angle distribution is due to the finite orbit width, finite Larmor radius, finite beam width and collisional scattering of the beam ions [17].

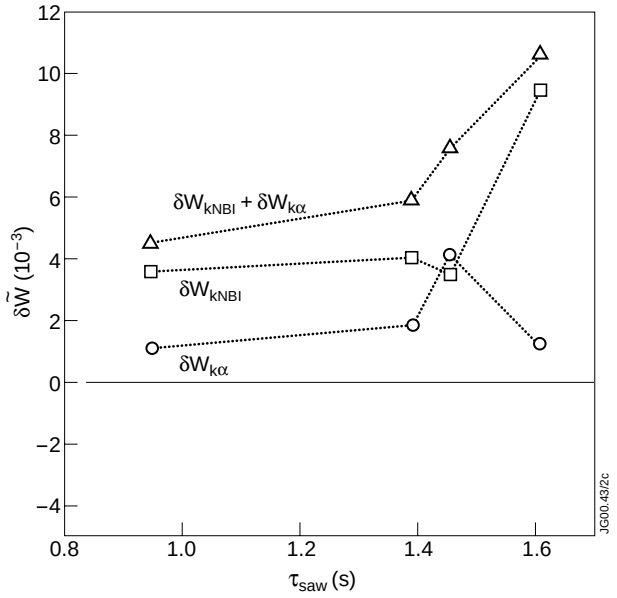

Figure 9: The open symbols show the calculated, $\delta W_{k\alpha}$ and δW_{kNBI} versus the sawtooth period using NOVA-K.

For the purpose of these calculations, we neglect plasma rotation. (Plasma rotation effects are discussed in a separate paper [24].) The radial NBI ion beta profile was taken from TRANSP. The results in Figure 9 show values computed using NOVA-K for δW_{kNBI} and $\delta W_{k\alpha}$ versus sawtooth period.

The two methods of calculation give almost identical values of δW_{kNBI} in two discharges. The analytical approach gives somewhat lower values of $\delta W_{k\alpha}$, but the overall effect of this on the kinetic part of the kink energy is small, since the dominant contribution comes from δW_{kNBI}. Note that we have excluded from the comparison the discharge with 100% T since the q-profile it has from TRANSP calculations is different from the other discharges. The eigenmode structure for this shot does not allow employing the perturbative analysis we use, which is based on the dispersion relation of Ref. [20].

We conclude that there is a positive correlation between the kinetic part of the kink energy and sawtooth period in the alpha-heating discharges. If we are justified in assuming that δW_{core} was approximately the same (at a given instant after the start of NBI) in every discharge, the correlation between kinetic kink energy and τ_{saw} is consistent with a scenario in which the occurrence of a sawtooth crash is delayed mainly by the presence of energetic ions (principally beam ions, in this case). Since the change in δW due to energetic ions is roughly proportional to the pressure of those ions, a progressive increase in the latter implies that δW_{core} must become progressively more negative in order for a sawtooth to be triggered [25]. The core kink energy is likely to fall during the course of the discharge, due to the combined effects of an increase in the total plasma pressure gradient and evolution of the q-profile. The latter process, particularly, is not likely to be strongly dependent on the beam pressure, and so the temporal evolution of δW_{core} should not have varied greatly from discharge to discharge. If the beam pressure is relatively high, however, δW_{core} will take a relatively long time to become sufficiently negative that Eq. (2) is satisfied: this is the most credible interpretation of the correlation in Figure 5. Increased sawtooth stability occurs essentially because of higher beam ion pressure, which in turn arises partly because of the fact that beam tritons are more massive than deuterons, and thus take longer to slow down.

4. ALPHA-PARTICLE EFFECT ON INTERNAL KINK STABILITY IN THE DISCHARGE WITH RECORD FUSION YIELD

We have also studied internal kink stability for the high performance DT discharges. Here we show the result of calculations for the record fusion discharge 42976 at the time of maximum P_{fus} = 16 MW (Figure 10). This discharge was obtained in the higher field configuration (details in Subsection 2.1). Similarly to the discharge with the highest P_{fus} in the standard configuration (discussed in Subsection 2.1) no sawtooth was observed.

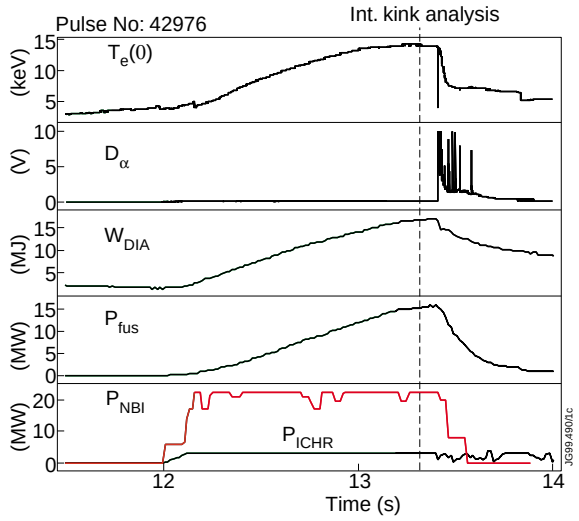

Figure 10: Time evolution for discharge where record fusion power was achieved. The time chosen for the analysis of the internal kink is indicated.

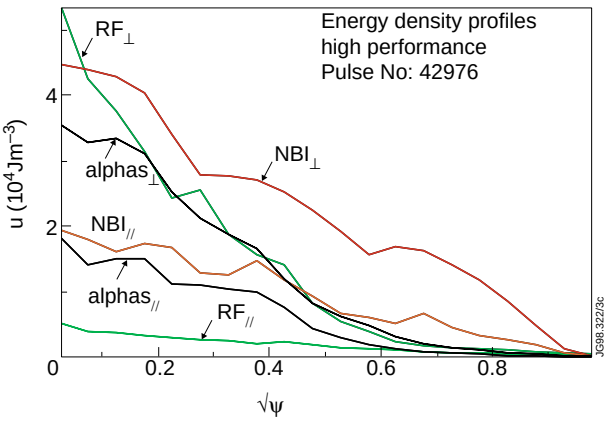

Figure 11: Profiles of beam and alpha-particles energy densities at time of record P_{fus} = 16MW (TRANSP t = 13.3 s)

Calculations were performed with the codes PEST [26] and NOVA-K [20] using TRANSP data. In the high performance discharges there were 3 types of fast ions: beam (η_T = 50%), ICRH (η_H = 1%) and alpha-particles, all with similar $u_\perp$ values (Figure 11). The contributions of these species to the kink mode damping rate are normalised to the Alfvén frequency, defined here as the core Alfvén speed divided by the product of the major radius and q_{95}. The normalised growth and damping rates γ/ω_A ($\propto \delta W$) are listed in Table 1, together with the corresponding beta toroidal. It is apparent from this table that the internal kink mode in this discharge was close to marginal stability. The alpha-particle stabilising contribution to δW_{kf} is of the same order as that arising from the ICRH minority H ions. The beam contribution, in contrast to the alpha-heating discharges discussed previously, is very small, despite the beam ions having energy densities comparable to those of the other energetic ion species. This may be due to a lower deuterium beam injection energy (76 keV), lower NBI beta and geometric factors, which decrease the ion toroidal precession drift frequency or effectively decreases beam ion energy. The most important conclusion to draw from Table 1 is that alpha-particles appear to have contributed substantially to sawtooth stabilisation in the highest performance JET DT discharges.

TABLE 1

Values of toroidal beta and normalised internal kink growth/damping rates in high performance DT discharge 42976.

	$\beta(0)$%	γ/ω_A %
MHD	5.81	-1.49
ICRH	0.65	+0.89
NBI (D)	0.25	-0.07
NBI (T)	0.44	+0.17
alpha-particles	0.6	+0.53
net growth/damping rate		+0.17

5. CONCLUSIONS

In a sequence of JET DT discharges designed to study alpha-heating there is a strong correlation between tritium fraction and the sawtooth period. We have shown that there is also a correlation between the kinetic energetic ion component of the m = 1 internal kink energy and the sawtooth period. In these discharges the main contribution to the kinetic kink energy is from beam ions rather than alpha-particles. Similar beam powers and injection energies were used in each of the alpha-heating discharges: the fast ion pressure nevertheless varied considerably from shot to shot, due partly to the mass dependence of the beam-ion slowing-down time and partly to a variation in the proportion of beam ions born at the full injection energy. Experimentally,

delaying sawtooth activity was found to be crucial in obtaining record fusion powers. Calculations have also shown that alpha-particles had a substantial stabilising effect on the m = 1 kink mode in the highest performance JET DT discharge, and may thus have delayed the occurrence of a sawtooth crash in that discharge.

ACKNOWLEDGEMENTS

We are grateful to R. Budny (PPPL), T. Hender, C. Gimblett (UKAEA) and J. Hastie (MIT) for helpful discussions. This work was funded partly by EURATOM, the UK Department of Trade and Industry, and the US Department of Energy.

REFERENCES

[1] Gibson A, and the JET Team, Plasma Physics **5** (1998) 1839.
[2] Keilhacker M, et al., Nuclear Fusion **39** (1998) 209.
[3] Thomas P et al., Physics Rev. Lett. **80** (1998) 5548.
[4] Nave M F F, et al., in Controlled Fusion and Plasma Physics (Proc. 25th Eur. Conf. Praha, 1998), Vol. 22C, European Physical Society, Geneva (1998) 365.
[5] Nave M F F, et al., Nuclear Fusion **39** (1999) 1567.
[6] Nave M F F, et al., Nuclear Fusion **35** (1995) 409.
[7] Alper B et al., in Controlled Fusion and Plasma Physics (Proc. 19th Eur. Conf. Innsbruck, 1992), Vol. 16C, Part I, European Physical Society, Geneva (1992) 331.
[8] The JET Team (presented by A Tanga), Plasma Physics and Controlled Fusion **36** (1994) B39.
[9] Nave M F F, et al., Nuclear Fusion **37** (1997) 809.
[10] Buttery R J et al., in Controlled Fusion and Plasma Physics (Proc. 26th Eur. Conf. Maastricht, 1999), Vol. 23J, European Physical Society, Geneva (1999) 121.
[11] Rimini F G, et al., Nuclear Fusion **39** (1999) 1591.
[12] Campbell D J et al., Phys. Rev. Lett. **60** (1988) 2148.
[13] Guo H Y, et al., Nuclear Fusion **40** (2000) 69.
[14] Porcelli F, Boucher D, Rosenbluth M N, Controlled Fusion and Plasma Physics 38 (1996) 2163.
[15] Lao L L, et al., Nuclear Fusion **30** (1990) 1035.
[16] Goldston, R J et al., J Comput. Phys. **43** (1981) 61
[17] Budny R V, Nucl. Fusion **34** (1994) 1247.
[18] Hemsworth, R S, in Plasma Physics and Nuclear Fusion Research, Academic Press, London (1981) 455.
[19] Rome, J A, McAlees, D G, Callen, J D, Fowler, R.H., Nuclear Fusion **16** (1976) 55.
[20] Cheng, C.Z., Phys. Reports **211** (1992) 1.

[21] Helander, P., Lisak, M., J. Plasma Physics **47** (1992) 281.

[22] McClements, K.G., Dendy, R.O., Gimblett, C.G., Hastie, R.J., Martin, T.J., Nucl. Fusion **35** (1995) 1761.

[23] Gorelenkov, N.N., Cheng, C.Z., Fu, G.Y., Phys. Plasmas **6** (1999) 2802.

[24] Gorelenkov, N.N., et al., in Controlled Fusion and Plasma Physics (Proc. 27th Eur. Conf. Budapest, 2000), to be published.

[25] Graves, J.P., Hopcraft, K.I., Dendy, R.O., Hastie, R.J., McClements, K.G.,Mantsinen, M., Phys. Rev. Lett. **84** (2000) 1204.

[26] Grimm, R., et al., Methods Comput. Phys. **16** (1976) 257.